PROCEEDINGS OF SCIENCE

Precision EWK and QCD measurements from ATLAS, CMS, LHCb

Valentina Guglielmi[1,*]

Deutsches Elektronen-Synchrotron (DESY),
Notkestrasse 85, Hamburg, Germany

E-mail: valentina.guglielmi@desy.de

These proceedings present a compilation of selected recent precise standard model (SM) measurements, including findings by ATLAS, CMS, LHCb. Covered topics include studies of quantum chromodynamics (QCD), such as the latest determinations of the strong coupling α_S, as well as the illustration of its running. Additionally, they include a status update on the precision measurements of the electroweak (EKW) physics. They present recent findings on W boson mass and width, as well as on the weak mixing angle. Additionally, the first determination of the τ lepton g-2 parameter in proton-proton collisions at the LHC is presented. These measurements are crucial for rigorous testing of the EWK and QCD sectors of the SM, and any deviations from the SM predictions could indicate the presence of new physics beyond the SM.

43rd International Symposium on Physics in Collision, PIC2024
22-25 October, 2024
Athens, Greece

[1] On behalf of the ATLAS, CMS and LHCb Collaborations
[*] Speaker

© Copyright owned by the author(s) under the terms of the Creative Commons Attribution-NonCommercial-NoDerivatives 4.0 International License (CC BY-NC-ND 4.0) All rights for text and data mining, AI training, and similar technologies for commercial purposes, are reserved. ISSN 1824-8039 . Published by SISSA Medialab.

PoS(PIC2024)062

1. Introduction

In these proceedings, a selection of recent results in electroweak (EWK) and quantum chromodynamics (QCD) standard model (SM) physics is presented, as available at the time of the PIC 2024 conference. These include results by ATLAS [1], CMS [2], and LHCb [3] Collaborations, performed with the data produced in proton-proton (pp) collisions at the LHC.

2. Precision tests of EWK physics

The parameters of the SM are interconnected with each other. For instance, the W boson mass, m_{W}, can be expressed as:

$$m_{\mathrm{W}} = \left(\frac{\pi\alpha_{\mathrm{EM}}}{\sqrt{2}G_{\mathrm{F}}}\right)^{1/2} \frac{\sqrt{1+\Delta R}}{\sin\theta_{\mathrm{W}}} \tag{1}$$

where α_{EM} is the fine-structure constant and G_{F} the Fermi coupling constant. Here, m_{W} is connected to the weak mixing angle θ_{W} and the radiative corrections ΔR, with the largest contributions from m_{t}^2 and $\ln(m_{\mathrm{H}})$. Precision measurements permit the testing of the self-consistency of the SM theory in global EWK fits, where possible tensions could be signs of beyond SM (BSM) phenomena. As a result, sensitivity to BSM effects can be achieved even if these phenomena would appear at an energy scale above what can be currently explored by direct searches.

2.1 W boson mass and width measurements

The most recent W boson mass measurement is from CMS [4], which uses a well-understood subset of $\sqrt{s} = 13$ TeV data (from the later part of 2016 data) and the muon decay channel of the W boson. The mass is extracted from a binned profile maximum likelihood fit to the three-dimensional distribution of the muon transverse momentum p_T^{μ}, pseudorapidity η^{μ}, and charge. This approach requires an extremely accurate and precise calibration of p_{T}^{μ}, which is directly sensitive to m_{W}, and a good understanding of the boson transverse momentum, $p_{\mathrm{T}}^{\mathrm{W}}$. The prefit measured and predicted $(p_{\mathrm{T}}^{\mu}, \eta^{\mu})$ distributions for positively charged muons are shown in Figure 1 (upper). At this stage, the systematic uncertainties are still large because no tuning has been performed on them yet. Figure 1 (lower) shows the postfit p_{T}^{μ} distribution. Thanks to the profiling of the systematics in the likelihood fit, now the size of the systematics uncertainties is drastically reduced. The final result is $m_{\mathrm{W}} = 80360.2 \pm 9.9$ MeV, which is the most precise determination at the LHC and with comparable precision to the CDF result [5]. The latest result from ATLAS comes from a re-analysis of the 2011 dataset [6], which features an improved extraction of m_{W} and the first determination of Γ_{W} at the LHC [7]. Separate measurements of mass and width are performed, as well as a simultaneous extraction. The m_{W} and Γ_{W} are measured from the p_{T}^{l} and $m_{\mathrm{T}}^{\mathrm{W}}$ distributions in $\mathrm{W} \to l\nu$ decays ($l = e/\mu$). The p_{T}^{l} distribution is shown in Figure 2 (left). An advanced physics model and a profile likelihood fitting procedure are used to reduce systematic uncertainties during the fit, leading to a reduction of about 15% of the total m_{W} uncertainty with respect to the previous result [6]. Additionally, this result includes the most precise single-experiment measurement of the W boson width, $\Gamma_{\mathrm{W}} = 2202 \pm 47$ MeV. Finally, the results of the simoultaneous extraction of m_{W} and Γ_{W} are illustrated in Figure 2 (right), together with their correlation. A combination of the W boson mass results from ATLAS, LHCb, CDF, and D0, as well as a compatibility study among them,

PoS(PIC2024)062

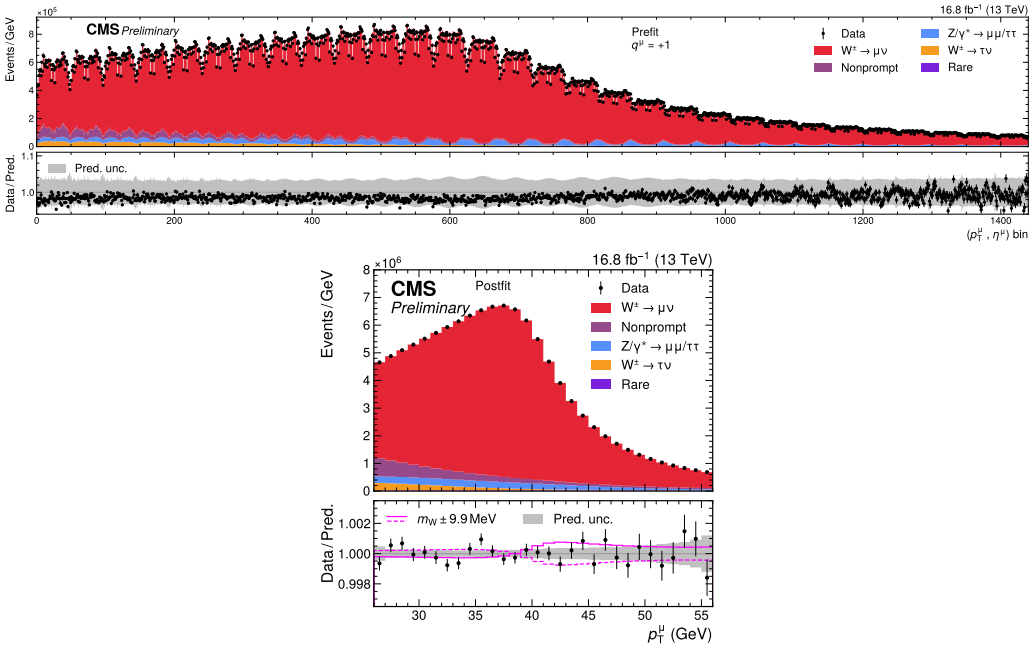

Figure 1: Upper: Measured and predicted $(p_{\mathrm{T}}^{\mu}, \eta^{\mu})$ distributions for positively charged muons from the CMS result [4]. The two-dimensional distribution is unrolled such that each bin on the x-axis represents one $(p_{\mathrm{T}}^{\mu}, \eta^{\mu})$ cell. The grey band represents the uncertainty in the prediction before the fit to the data. Lower: Measured and predicted p_{T}^{μ} distributions integrated into η and charge, with the prediction adjusted according to the best fit values of the nuisance parameters obtained from the maximum likelihood fit of the CMS result [4]. The solid and dashed pink lines represent, respectively, an increase and decrease of m_{W} by 9.9 MeV. The uncertainties in the predictions, after the systematic uncertainty profiling in the maximum likelihood fit, are shown by the shaded band. Images from Ref. [4].

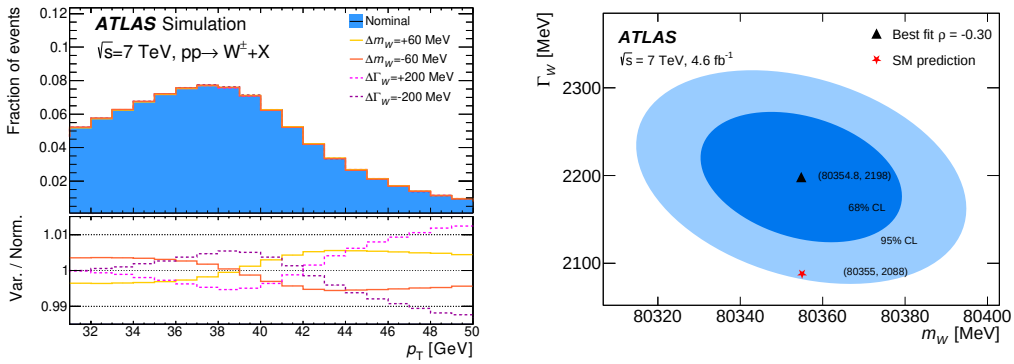

Figure 2: Left: The ATLAS simulated kinematic distributions of p_{T}^{l} in $\mathrm{W} \rightarrow \mu\nu$, for W-boson mass and width values of m_{W} = 80399 MeV and Γ_{W} = 2085 MeV. The ratio panel represents the relative effect of varying these parameters by ±60 MeV and ±200 MeV, respectively. Image taken from Ref. [7]. Right: 68% and 95% CL uncertainty contours for the simultaneous determination of m_{W} and Γ_{W} using the CT18 PDF set from ATLAS result [7]. The triangular marker represents the best fit, while the star corresponds to the SM prediction. Image taken from Ref. [7].

PoS(PIC2024)062

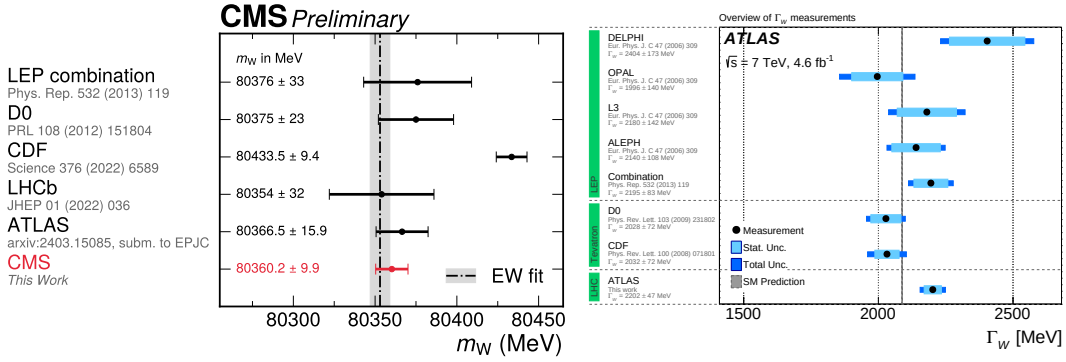

Figure 3: Summary of the W boson mass (left) and width (right) measurements. Images taken from Ref. [4] and Ref. [7], respectively.

is presented in [8]. The ATLAS result used in this combination is the original one from [6]. The combinations were also performed by removing each measurement individually. A high probability of compatibility is observed when removing the CDF measurement from the combination. In this case, the W boson mass from the combination results to be $m_{\mathrm{W}} = 80369.2 \pm 13.3$ MeV [8]. Figure 3 shows a comparison of the different W boson mass (left) and width (right) results.

2.2 Determinations of the EWK mixing angle

At the heart of the standard model the EWK mixing angle is described by $\sin^2\theta_{\mathrm{W}} = 1 - m_{\mathrm{W}}^2/m_{\mathrm{Z}}^2$, while at higher orders the effective weak mixing angle $\sin^2\theta^l_{\mathrm{eff}} = k_f \cdot \sin^2\theta_{\mathrm{W}}$ is introduced, where k_f is a flavour-dependent effective scaling factor absorbing higher order corrections. At the LHC, the effective mixing angle (leptonic) is measured with Drell-Yan events in the Collin-Soper frame [9]. The final state lepton angular distribution can be written as:

$$\frac{\mathrm{d}\sigma}{\mathrm{d}\cos\theta} \sim 1 + \cos^2\theta + \frac{1}{2}\mathrm{A}_0(1 - 3\cos^2\theta) + \mathrm{A}_4\cos\theta \tag{2}$$

where the linear term A_4 is sensitive to the forward-backward asymmetry $A_{\mathrm{FB}} = 3/8A_4$, and hence to $\sin^2\theta^l_{\mathrm{eff}}$. The most precise determinations of $\sin^2\theta^l_{\mathrm{eff}}$ are from LEP and SLD [10]. Recently, both CMS [11] and LHCb [12] determined $\sin^2\theta^l_{\mathrm{eff}}$. Both experiments performed a rapidity-dependent measurement to solve the ambiguity in the quark direction. In CMS, the reconstruction of muons is performed up to $|\eta| < 2.4$, which is the nominal acceptance of the tracker, while the one of electrons is extended up to $|\eta| < 4.36$ exploiting the larger coverage of the calorimeters. In the LHCb measurement, the high quality of muon reconstruction covers $2 < \eta < 4.5$. The forward-backward asymmetry is shown in Figure 4 (left) and Figure 5 (left) for CMS and LHCb, respectively. The parton distribution functions (PDFs) represent the largest expected contribution to the uncertainty of the CMS measurement, and have been profiled in the fit. The reduction of the uncertainty, before and after profiling, can be appreciated in Figure 4 (right). In CMS also the unfolded A_4 distribution has been measured and used to extract $\sin^2\theta^l_{\mathrm{eff}}$, useful for reinterpretations in the future. In LHCb no profiling was needed since the uncertainty is dominated by the statistics.

PoS(PIC2024)062

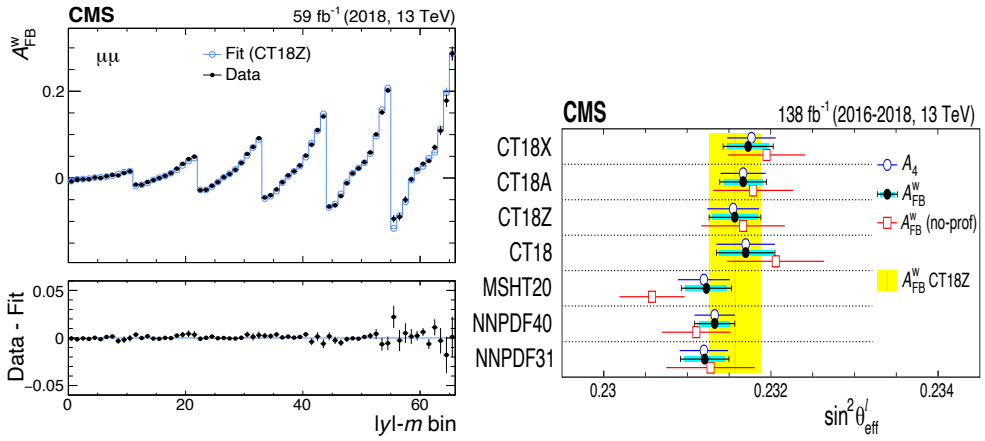

Figure 4: Left: Measured and best fit $A_{\mathrm{FB}}^{\mathrm{W}}(|y|, m)$ distributions in the $\mu\mu$ channel from the CMS result [11]. The error bars represent the statistical uncertainties in the measured and simulated samples. Right: Values of $\sin^2\theta^l_{\mathrm{eff}}$ measured with $A_{\mathrm{FB}}^{\mathrm{W}}$ and A_4 fits for seven PDF sets from the CMS result [11]. The orange line and yellow band correspond to the result obtained with the CT18Z PDFs. The red open squares are the results obtained without profiling the corresponding PDF uncertainties. For the $A_{\mathrm{FB}}^{\mathrm{W}}$ results, the cyan bands show the PDF uncertainties and the black bars represent the total uncertainties. Images from Ref. [11].

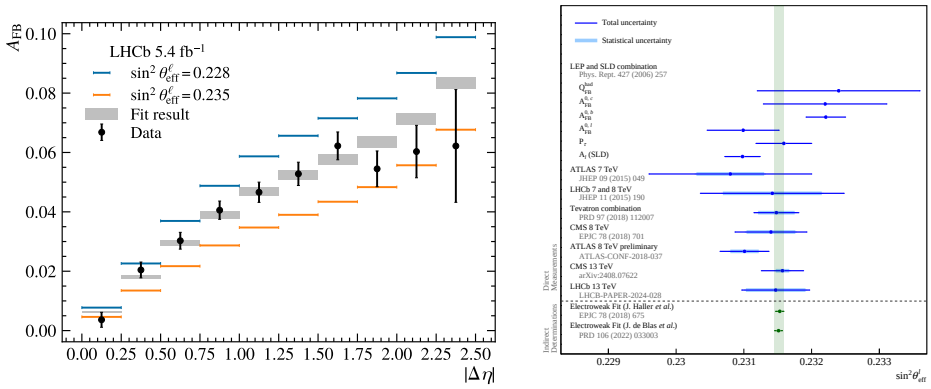

Figure 5: Left: Measured A_{FB} in ten intervals of $\Delta\eta$, with the results of the $\sin^2\theta^l_{\mathrm{eff}}$ fit from the LHCb result [12]. The grey band shows the fit result and the associated statistical uncertainty. Right: Summary of the determinations of the weak mixing angle. Images from Ref. [12].

Promising prospects are indeed expected for Run3. The final results are:

$$\begin{aligned} \text{CMS}: \ \sin^2\theta^{\mathrm{l}}_{\mathrm{eff}} &= 0.23157 \pm 0.00010(\mathrm{stat}) \pm 0.00015(\mathrm{syst}) \pm 0.00009(\mathrm{theo}) \pm 0.00027(\mathrm{PDF}) \\ \text{LHCb}: \ \sin^2\theta^{\mathrm{l}}_{\mathrm{eff}} &= 0.23147 \pm 0.00044(\mathrm{stat}) \pm 0.00005(\mathrm{syst}) \pm 0.00023(\mathrm{theo/PDF}) \end{aligned} \tag{3}$$

where the CMS result is the most precise determination at hadron colliders. These results are summarised and compared with previous determinations in Figure 5 (right).

PoS(PIC2024)062

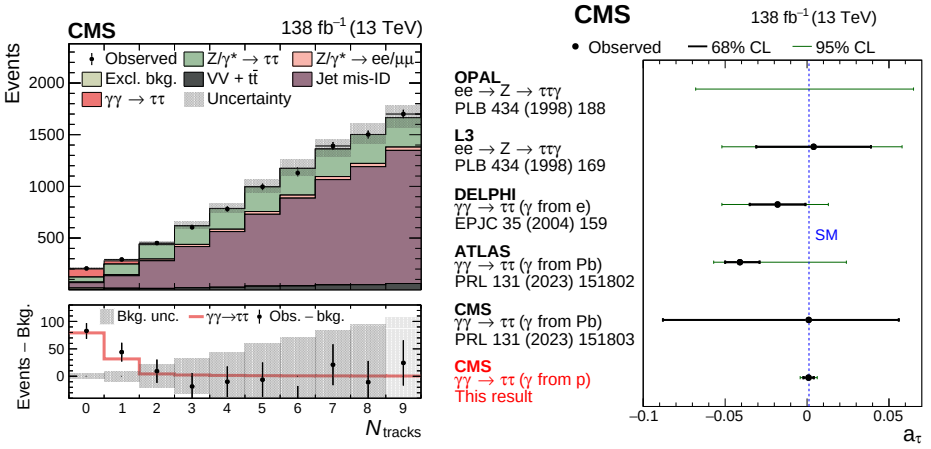

Figure 6: Left: Illustration of the isolated signal at low track multiplicity from the CMS result [13]. Right: Summary of measurements of a_τ. Images from Ref. [13].

3. First measurement of τ lepton g-2 in pp collisions

Particles with spin S have a magnetic moment μ. For spin-1/2 particles, quantum corrections with a gyromagnetic factor g need to be considered, with $g \approx 2.00232$. The anomalous magnetic moment a is defined as the deviation of g from the exact value of 2 predicted by the Dirac theory, $a = \frac{g-2}{2}$. While $(g-2)_e$ is measured in Penning traps and $(g-2)_\mu$ in storage rings, $(g-2)_\tau$ can be constrained in particle collisions (pp or PbPb). The recent result from CMS is the first observation of $\gamma\gamma \to \tau\tau$ production in pp collisions [13]. In this measurement, the protons remain intact or fragment out of the detector acceptance. As a consequence, no other particles are reconstructed in CMS except for the decay products of the τ. This results in an isolated signal at low track multiplicity, as shown in Figure 6 (left). In this measurement, the $(g-2)_\tau$ is probed with unprecedented precision. The final result is $a_\tau = \frac{g_\tau}{2} - 1 = 0.0009^{+0.0016}_{-0.0015}\ (\text{syst})^{+0.0028}_{-0.0027}\ (\text{stat})$, representing the most precise measurement to date, as shown in Figure 6 (right). Since the total uncertainty is dominated by the statistics, promising improvements are expected from the extension of the analysis to the additional data from the still ongoing Run3 of the LHC.

4. Precision tests of QCD physics

The strong coupling α_S is the only free parameter of QCD in the limit where quark masses go to zero. Additionally, it plays a crucial role in determining the stability of the electroweak vacuum [14] and in the context of the Grand Unified Theory [15]. Despite significant improvements in its precision over recent years, α_S remains the least known coupling among all fundamental interactions. Consequently, it is crucial to refine its determination further, as its uncertainty constitutes one of the primary sources of uncertainty in many precision measurements, such as the Higgs boson couplings at the LHC. The strong coupling constant $\alpha_S(m_Z)$ can be determined from the factorisation theorem at the LHC by comparing the experimental cross section measured in data to the partonic cross section computed in perturbative QCD and convoluted with the PDFs. The ATLAS result [17], based on the precise measurement of the Z boson p_T distribution at $\sqrt{s} = 8$ TeV [16], illustrated

PoS(PIC2024)062

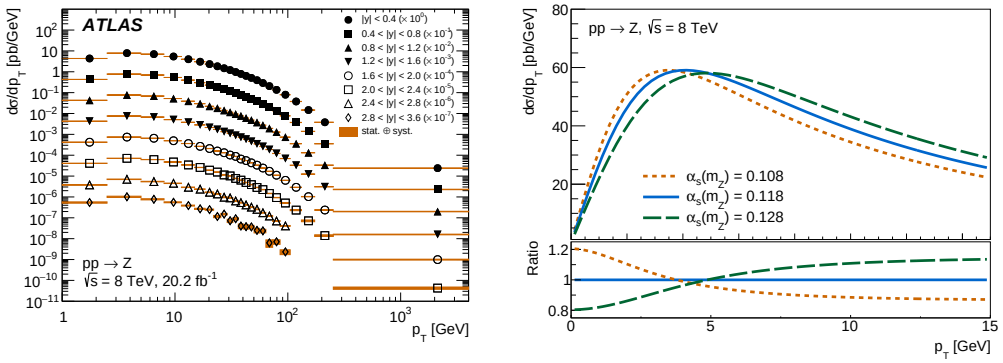

Figure 7: Left: Measurement of Z p_{T} spectrum from the ATLAS result [16]. Right: Sensitivity of Z p_{T} spectrum to $\alpha_S(m_{\mathrm{Z}})$ used for its determination, from the ATLAS result [17].

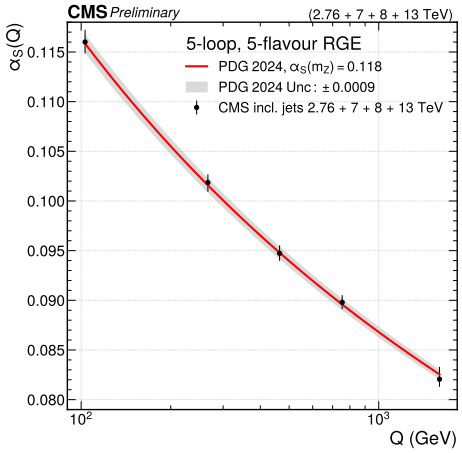

Figure 8: Illustration of the α_S running at NNLO accuracy from the CMS result [18].

in Figure 7 (left), is the most precise experimental determination of $\alpha_S(m_{\mathrm{Z}})$ to date. The rationale for the measurement is that Z bosons recoil against QCD initial-state radiation, leading to the position of the peak of the Z boson p_{T} spectrum being highly sensitive to $\alpha_S(m_{\mathrm{Z}})$, as shown in Figure 7 (right). The final result is $\alpha_S(m_{\mathrm{Z}}) = 0.1183 \pm 0.0009$ obtained at N^{4}LLa+N^{3}LO QCD accuracy. The last recent determination of $\alpha_S(m_{\mathrm{Z}})$ is performed by the CMS experiment using double-differential cross section measurements of inclusive jet production at $\sqrt{s}$ = 2.76, 7, 8, and 13 TeV. The value of the strong coupling $\alpha_S(m_{\mathrm{Z}})$ is determined in a comprehensive analysis at NNLO order accuracy in QCD, where a simultaneous extraction of PDFs and $\alpha_S(m_{\mathrm{Z}})$ is performed to mitigate their correlation and avoid a potential bias in the determination of $\alpha_S(m_{\mathrm{Z}})$ [19]. The final result, $\alpha_S(m_{\mathrm{Z}}) = 0.1176^{+0.0014}_{-0.0016}$, is the most precise from jets [18]. By using the measurements in different intervals of jet p_{T}, the running of α_S has also been probed for energies between 100 and 1600 GeV. The running of α_S is shown in Figure 8. Many other results characterised the last past few years both at NLO and NNLO accuracy [20–24].

PoS(PIC2024)062

5. Summary and Conclusions

Recent results at the LHC have achieved remarkable precision, often surpassing initial expectations. Large datasets, detailed understanding of the detectors, and dedicated reconstruction techniques, coupled with state-of-the-art theory predictions, have enabled stringent tests of the SM with numerous results in the last 12 months. Novel ideas and methods are continuously developed. Precision measurements of EWK and QCD parameters play a crucial role in determining the extent to which the SM accurately describes the physical world and pave the way towards future research at colliders.

References

[1] ATLAS Collaboration, *The ATLAS Experiment at the CERN Large Hadron Collider* JINST, **3**, (2008) S08003.

[2] CMS Collaboration, *The CMS experiment at the CERN LHC* JINST, **3**, (2008) S08004.

[3] LHCb Collaboration, *The LHCb Detector at the LHC* JINST, **3**, (2008) S08005.

[4] CMS Collaboration, *High-precision measurement of the W boson mass with the CMS experiment at the LHC*, arXiv:2412.13872.

[5] CDF Collaboration, *High-precision measurement of the* W *boson mass with the CDF II detector*, *Science*, **376**, (2022) 6589.

[6] ATLAS Collaboration, *Measurement of the* W*-boson mass in pp collisions at* $\sqrt{s} = 7$ *TeV with the ATLAS detector*, *EPJC*, **78**, (2018) 898.

[7] ATLAS Collaboration, *Measurement of the W-boson mass and width with the ATLAS detector using proton-proton collisions at* $\sqrt{s} = 7$ *TeV*, *EPJC*, **84**, (2024) 12, arXiv:2403.15085.

[8] LHC-TeV MW Working Group, *Compatibility and combination of world W-boson mass measurements*, *EPJC*, **84**, (2024) 451 [arXiv:2308.09417].

[9] J. C. Collins, and D. E. Soper, *Angular Distribution of Dileptons in High-Energy Hadron Collisions*, *PRD*, **16**, (1977) 2219.

[10] ALEPH, DELPHI, L3, OPAL, SLD, LEP Electroweak Working Group, SLD Electroweak Group, SLD Heavy Flavour Group *Precision electroweak measurements on the Z resonance*, *PR*, **427**, (2006) 257.

[11] CMS Collaboration, *Measurement of the Drell–Yan forward-backward asymmetry and of the effective leptonic weak mixing angle in proton-proton collisions at* $\sqrt{s} = 13$ *TeV*, arXiv:2408.07622.

[12] LHCb Collaboration, *Measurement of the effective leptonic weak mixing angle*, *JHEP*, **12**, (2024) 026 [arXiv:2410.02502].

PoS(PIC2024)062

[13] CMS Collaboration, *Observation of $\gamma\gamma \to \tau\tau$ in proton-proton collisions and limits on the anomalous electromagnetic moments of the τ lepton*, *RPP*, **87**, (2024) 107801 [arXiv:2406.03975].

[14] G. Degrassi, S. Di Vita, J. Elias-Miro, J. R. Espinosa, G. F. Giudice, G. Isidori, and A. Strumia, *Higgs mass and vacuum stability in the Standard Model at NNLO*, *JHEP*, **08**, (2012) 098 [arXiv:1205.6497].

[15] A. Bartl, and S. Hesselbach, *Standard model and beyond*, arXiv:hep-ph/0412419.

[16] ATLAS Collaboration, *A precise measurement of the Z-boson double-differential transverse momentum and rapidity distributions in the full phase space of the decay leptons with the ATLAS experiment at $\sqrt{s} = 8$ TeV*, *EPJC* **84** (2024) 315 [arXiv:2309.09318].

[17] ATLAS Collaboration, *A precise determination of the strong-coupling constant from the recoil of Z bosons with the ATLAS experiment at $\sqrt{s} = 8$ TeV*, arXiv:2309.12986.

[18] CMS Collaboration, *The strong coupling constant and its running from inclusive jet production at CMS*, CMS-PAS-SMP-24-007.

[19] S. Forte and Z. Kassabov, *Why α_s cannot be determined from hadronic processes without simultaneously determining the parton distributions*, *EPJC*, **80**, (2020) 182 [arXiv:2001.04986].

[20] CMS Collaboration, *Measurement and QCD analysis of double-differential inclusive jet cross sections in proton-proton collisions at $\sqrt{s} = 13$ TeV*, *JHEP*, **02**, (2022) 142, Addendum: *JHEP* **12**, (2022) 035 [arXiv:2111.10431].

[21] CMS Collaboration, *Measurement of multidifferential cross sections for dijet production in proton-proton collisions at $\sqrt{s} = 13$ TeV*, arXiv:2312.16669.

[22] CMS Collaboration, *Measurement of energy correlators inside jets and determination of the strong coupling $\alpha_S(m_Z)$*, *PRL*, **133**, (2024) 071903 [arXiv:2402.13864].

[23] CMS Collaboration, *Measurement of multijet azimuthal correlations and determination of the strong coupling in proton-proton collisions at $\sqrt{s} = 13$ TeV*, *EPJC*, **84**, (2024) 842 [arXiv:2404.16082].

[24] ATLAS Collaboration, *Determination of the strong coupling constant from transverse energy–energy correlations in multijet events at $\sqrt{s} = 13$ TeV with the ATLAS detector*, *JHEP*, **07**, (2023) 085 [arXiv:2301.09351].

PoS(PIC2024)062